Mechanical Systems and Signal Processing 111 (2018) 570–579

Contents lists available at ScienceDirect

Mechanical Systems and Signal Processing

journal homepage: www.elsevier.com/locate/ymssp

Damage detection in pipes based on acoustic excitations using laser-induced plasma

Itsuro Kajiwara [a,*], Ryosuke Akita [a], Naoki Hosoya [b]

[a] Division of Human Mechanical Systems and Design, Hokkaido University, N13, W8, Kita-ku, Sapporo 060-8628, Japan
[b] Department of Engineering Science and Mechanics, Shibaura Institute of Technology, 3-7-5 Toyosu, Koto-ku, Tokyo 135-8548, Japan

ARTICLE INFO

Article history:
Received 17 September 2017
Received in revised form 16 February 2018
Accepted 5 April 2018

Keywords:
Laser-induced plasma
Acoustic excitation
Health monitoring
Damage detection
Wavelet transform

ABSTRACT

A health-monitoring system is proposed to detect holes drilled in a pipe based on laser plasma acoustic excitations and acoustic measurements. In this system, an acoustic excitation is applied to a pipe via a laser-induced plasma in air generated by a high-power Nd:YAG pulse laser. Laser-induced plasmas can realize non-contact acoustic impulse excitations. A microphone is used to measure the time response of the acoustic pressure. In this study, we focus on the detection of a hole in the pipe. The reflection of the acoustic wave due to a hole drilled in the pipe induces a change in the time response of the acoustic pressure. Applying a continuous wavelet transform to the measured time response data with/without the hole can locate the position of the hole. This study demonstrates the effectiveness of the present damage detection method based on an acoustic excitation using a laser-induced plasma.

1. Introduction

To prevent accidents due to structural failures, machine conditions must be regularly monitored. Vibration-based health monitoring approaches are actively studied in various damage detection fields such as crack/failure detection in a structure and bolted joint loosening detection. In these studies, vibration/acoustic data are measured by a sensor, which includes an accelerometer and microphone, under excitation with an impulse hammer and a piezoelectric actuator or a speaker. Additionally, fiber optic sensors are commonly used for structural health monitoring in various mechanical systems, including aircraft composite structures [1].

In recent years, health monitoring of infrastructure (e.g., roads, bridges, and pipelines) has received increased attention because effective maintenance of aging infrastructure is imperative to ensure safe and reliable structures. Several approaches have been investigated to detect the loosening of bolted joints. These include using impedance [2,3], electrical conductivity [4], and vibration measurements [5]. Vibration-based approaches commonly involve contact excitations using piezoelectric materials or impulse hammers to excite a structure and determine the frequency response. However, the excitation device must be firmly attached to the structure to use piezoelectric components. Larger sized piezoelectric components may need to be bolted to the structure. Hammering methods require specially trained technicians and are time consuming. Although dynamic characteristic measurements must be highly reproducible to be useful, the reproducibility of the input characteristics with a hammer is poor. These issues have led to research into non-contact excitation methods with a better reproducibility [6].

* Corresponding author.
E-mail addresses: ikajiwara@eng.hokudai.ac.jp (I. Kajiwara), ryosuke-akita@frontier.hokudai.ac.jp (R. Akita), hosoya@sic.shibaura-it.ac.jp (N. Hosoya).

https://doi.org/10.1016/j.ymssp.2018.04.004
0888-3270/

Acoustic excitation with a speaker can effectively realize non-contact excitation with a high reproducibility. Several methods have been proposed to generate impulse sound sources, including those employing speakers [7], a spark discharge [8], and a wire explosion [9]. However, these methods require device (e.g., speakers and wires) setup in a sound field, which may disturb the sound field. Moreover, the setup is extremely difficult when the sound field is inside a closed container or filled with materials harmful to humans like carbon dioxide. In research on damage detection in pipes, approaches using ultrasonic guided waves [10–12] and pattern recognition techniques [13] have been investigated. These techniques require that the excitation and measurement devices are attached to the structures.

We have realized an ideal point excitation using a laser excitation method based on laser ablation (LA) [14–20], but the LA-generated excitation induces sub-millimeter-sized damage onto the laser-irradiated surface of a structure. From the viewpoint of non-contact and non-destructive acoustic excitations, several methods using a point sound source generated by a laser-induced plasma (LIP) have been proposed for acoustic tests [21–24]. The LIP is a phenomenon where electrons emitted from atoms and molecules that absorb multiple injected photons produce a plasma via a focused laser beam into a gas.

Many studies have investigated LIPs [25]. For example, ignition with a laser spark [26], LIP spectroscopy [27], and LIP in water [28]. Accurate frequency characteristics have been measured by LIP excitations [29–31]. This approach has been applied to evaluate the firmness of apples [32] and to detect damage in membrane structures [33]. It is expected that combining an LIP acoustic excitation and a health monitoring approach will enhance the efficiency and accuracy of damage detection because excitation devices do not need to be placed in an acoustic field or on the structure.

Herein a damage detection system is demonstrated on the basis of an LIP acoustic excitation and acoustic measurements assuming that a hole drilled on a pipe structure induces damage. This excitation method has the following advantages. First, the excitation force can be applied in a non-contact manner without placing an excitation device such as an exciter or actuator on the target. This is beneficial because placing a device on the target may change the dynamic characteristics of the target structure. In the present technique, an excitation force is provided in a non-contact manner. Second, a high reproducibility can be achieved. The reproducibility of the excitation force in the hammering excitation method depends largely on the skills on the person conducting the measurements. Hence, reproducibility is difficult. On the other hand, a high degree of reproducibility can be assured using a laser excitation method since the excitation force defined by the laser energy is applied.

In the present system, the time history response of the sound pressure is collected by acoustic excitations via an LIP and acoustic measurements by a microphone using an acrylic pipe as the target structure. A continuous wavelet transform is applied to the time variation of the sound pressure inside the pipe, and extracting the reflected waves through the damaged hole identifies the damaged position. Experiments demonstrate that this method effectively and accurately identifies the damaged position.

2. Acoustic excitation via LIP

An LIP refers to a phenomenon where focusing a laser beam onto a gas causes atoms or molecules to absorb many photons by a multiphoton process. Then electrons are emitted and a plasma is formed via a cascade process. The shockwaves formed by converting part of the plasma energy at this time become the sound source via the LIP [29–31].

Previously, the sound pressure when an LIP is generated was measured using a microphone (Fig. 1) to evaluate the acoustic excitation characteristics [29]. For the time history response waveforms of the sound pressure for a point sound source via an LIP, Fig. 2 shows a diagram with an enlarged time axis around the sound pressure generation point. Fig. 3 shows the corresponding Fourier spectrum. Fig. 2(a)–(c) shows the results when the focal length l_f of a lens is 100 mm

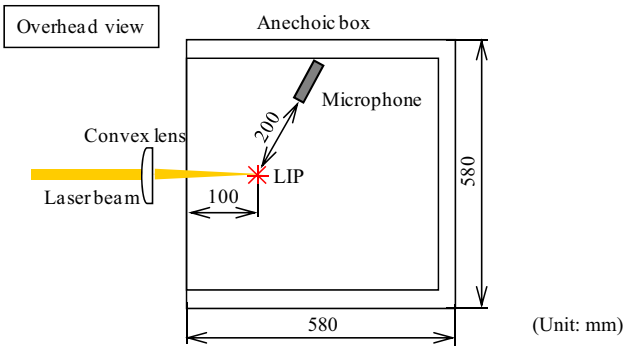

Fig. 1. Acoustic excitation by LIP [29].

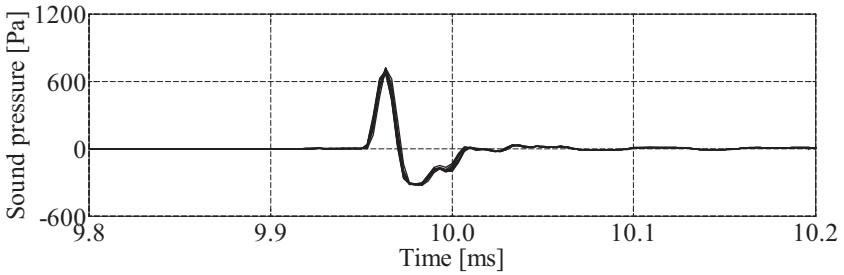

(a) Convex lens L1 (l_f = 100 mm) (average of peak sound pressure: 698.9 Pa)

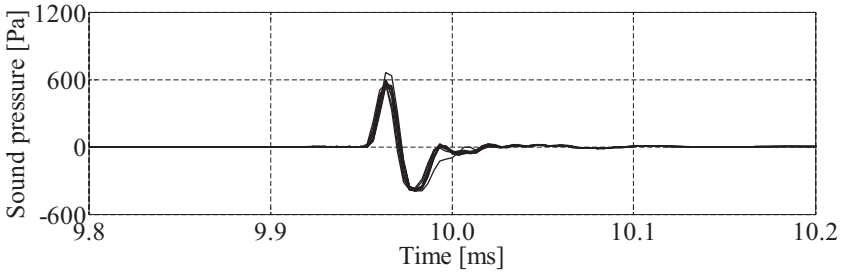

(b) Convex lens L2 (l_f = 200 mm) (average of peak sound pressure: 577.1 Pa)

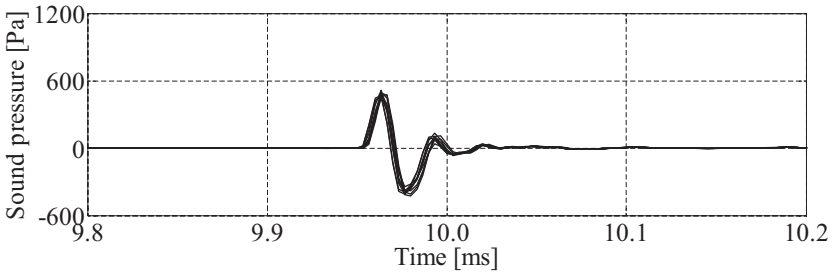

(c) Convex lens L3 (l_f = 300 mm) (average of peak sound pressure: 480.3 Pa)

Fig. 2. Time responses of sound pressure generated by LIP (energy E = 335.9 mJ) [29].

(L1), 200 mm (L2) and 300 mm (L3), respectively. The results from ten measurements overlap. The point sound source generated via an LIP has a pulse width of 20 μs, which is almost an ideal impulse force that includes components up to the high frequency band of about 100 kHz. In addition, appropriately setting the laser energy or the focal length of a convex lens ensures the reproducibility of the sound pressure of the point sound source via an LIP (Fig. 2). Unlike LA, the advantage of the LIP excitation method is that a complete non-contact excitation can be realized since the laser is not directly irradiated onto the measurement target. Furthermore, according to the acoustic characteristics in Figs. 2 and 3, the sound pressure level measured 200 mm away from the sound source exceeds 70 dB in the audible frequency band. In this study, if sound propagating in a pipe is assumed to be a plane wave, sound attenuation is theoretically very small, and an acoustic excitation force can effectively measure the acoustic characteristics in a sound field inside the pipe by the LIP.

3. Objective structure and experimental system

The target structure is an acrylic pipe. The pipe has an outer diameter of 22 mm, an inner diameter of 20 mm, and an overall length of 1000 mm. Figs. 4 and 5 show the overall view and a schematic view of the acoustic excitation and measurement system using a laser, respectively. The experimental apparatus consists of a Nd: YAG laser (Surelite III-10, Continuum, wavelength of 1064 nm, laser beam radius of 4.75 mm, pulse width of 5 ns, maximum output of 850 mJ, and radial divergence angle of 0.25 mrad), convex lens (focal length of 100 mm), acrylic pipe, microphone (UC-54, RION, measurement frequency range of 20 Hz–100 kHz), and spectrum analysis system (A/D; NI PXI-1042Q, PXI-4472B, Software; CAT-System CATEC).

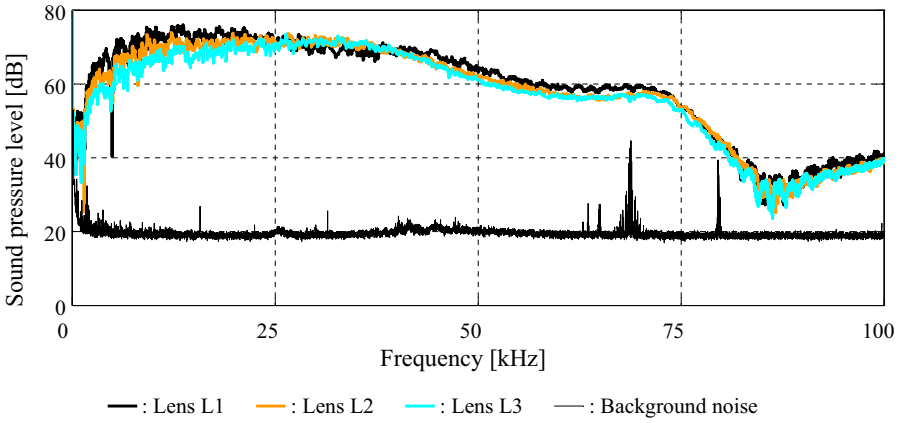

Fig. 3. Fourier spectra of sound pressure generated by LIP for three convex lenses [29].

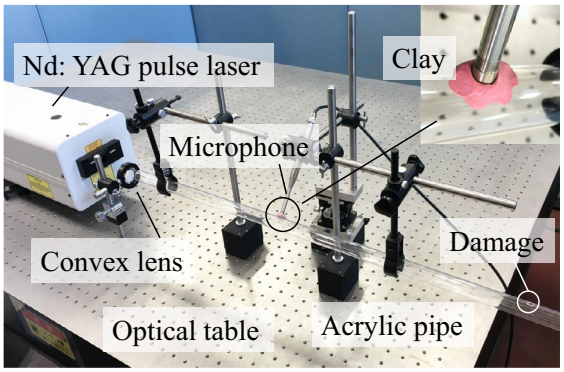

Fig. 4. Overview of the experimental system.

The laser light emitted from YAG laser is focused into a pipe by a convex lens to generate an LIP. Consequently, a point sound source via the LIP is generated and the inner part of the pipe is acoustically excited. Here, when the LIP is generated in the air, most of the laser energy is converted in the air. Thus, the influence of irradiation laser such as damaging the pipe structure is negligible. Then the sound waves propagating through the pipe are measured by a microphone attached to the pipe, and the time history response of the sound pressure is collected. The position of the acoustic excitation point is set to a point 50 mm from the entrance of the pipe. The measurement position by the microphone is set 350 mm from the entrance.

In the present experimental apparatus, with respect to acoustic measurement, a hole is made in the pipe and the microphone is inserted. There is a slight gap between the microphone and the pipe. To reduce the influence on the sound field, the gap is filled with clay. As far as the measured acoustic characteristics described below are concerned, the influence of the installed microphone on the sound field can be ignored. On the other hand, even if the acoustic characteristics change due to installation of the microphone, the abnormality detection method described in Section 4 can be applied provided that a normal state and an abnormal state are defined. Applying a continuous wavelet transform to the measured acoustic data and extracting minor changes in the sound pressure characteristics successfully detects damage and identifies the damaged location.

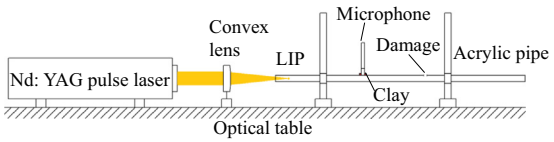

Fig. 5. Schematic of the experimental system with an LIP.

4. Wavelet transform for damage detection

Wavelet transform is a frequency analysis method. This method can conserve time-domain information, which is lost during a Fourier transform. Using a base of conversion called the mother wavelet, the extent of the mother wavelet in the signal is analyzed and the results are outputted as a wavelet coefficient. The wavelet coefficient increases as the portion of the signal agrees with the wavelet of a certain scale and at a certain location. However, the coefficient becomes smaller when the correlation is insufficient [33]. In this study, a one-dimensional continuous wavelet transform is used to detect damage.

4.1. Mother wavelet

The mother wavelet is the base of a wavelet transform. Scaling and a parallel translation of a mother wavelet are performed and applied to the signal to be analyzed. The signal is processed by checking the correlation. The present study adopts the Mexican hat wavelet, which is a famous continuous wavelet transform that does not include a complex function. The Mexican hat wavelet is shown in Eq. (1).

$$\psi(t) = (1 - t^2)e^{-\frac{t^2}{2}} \tag{1}$$

To apply the mother wavelet to the signal analysis, $\psi(t)$ in Eq. (1) must be converted into a form that allows for more flexible scaling and parallel translation. For scaling, a scale parameter a is used for the mother wavelet, whereas a shift parameter b is used for the parallel translation. Eq. (2) gives the Mexican hat wavelet in a form that considers the parallel translation and scaling.

$$\psi\left(\frac{t-b}{a}\right) = \left\{1 - \left(\frac{t-b}{a}\right)^2\right\} e^{-\frac{1}{2}\left(\frac{t-b}{a}\right)^2} \tag{2}$$

The original mother wavelet represented by Eq. (1) is when $a = 1$ and $b = 0$. Based on Eq. (2), the two parameters a and b are varied to transform the signal to be analyzed.

4.2. Continuous wavelet transform

The continuous wavelet transform for a one-dimensional function is given by Eq. (3).

$$W(a,b) = \frac{1}{\sqrt{a}} \int_{-\infty}^{\infty} x(t)\psi\left(\frac{t-b}{a}\right)dt \tag{3}$$

Here, $W(a,b)$ is the wavelet coefficient, and $x(t)$ is the signal to be analyzed and represents the time history response of the sound pressure variation inside the pipe. Scale parameter a of the wavelet is proportional to frequency f. Frequency f is referred to as the characteristic frequency, and is typically given by Eq. (4).

$$f = \frac{f_c}{a} \tag{4}$$

Here, f_c is the center frequency of the mother wavelet pass band. For the Mexican hat wavelet, $f_c = 0.25$ Hz [34].

4.3. Extraction of the characteristic change due to damage

Fig. 6 schematically diagrams the phenomenon that occurs inside a pipe with a hole when an LIP is generated near the entrance of the pipe. Additionally, an acoustic traveling wave is generated. After that, the acoustic traveling wave is reflected repeatedly at the end of the pipe but shifts to a stationary wave. Besides the reflection at the end of the pipe, the acoustic wave should be slightly reflected at the damaged part on the pipe. This reflection can be measured by the microphone.

Detection of damage and identification of the damaged position are considered by capturing the reflected wave from this damaged part from the measured data. The time when the acoustic traveling wave is first measured by the microphone is t_1. The wave propagates in its original form until it reaches the hole. Afterwards, the wave is divided into a wave reflected by the damage and continues to propagate. The reflected wave is again measured by the microphone at t_2. If the time when the sound wave is first measured at t_1 and the time when the reflected wave is measured at t_2 are determined, the distance from the microphone to the hole can be calculated by multiplying the difference of these times by the speed of sound. However, the effect of the sound wave reflected by microscopic damage should be much smaller than the initially generated acoustic traveling wave and the sound wave reflected at the end of the pipe. By applying a continuous wavelet transform to the measured acoustic data and extracting the slight change in the sound pressure data caused by the reflected wave due to the damage, t_1 and t_2 can be identified. Consequently, both the presence of damage and its position can be determined.

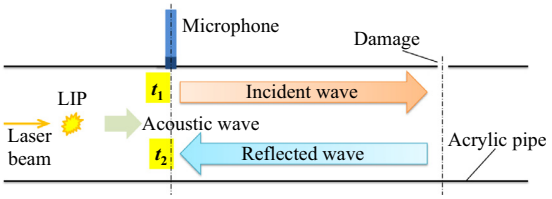

Fig. 6. Schematic diagram of the wave reflection at a damaged position.

5. Results and discussion

5.1. Acoustic characteristics in the normal condition

The acoustic characteristics inside the pipe are measured using the experimental apparatus described in Section 3. The acoustic excitation is performed with a laser output of 600 mJ, while the sound pressure data is measured by a microphone. The location of the LIP is 50 mm from the entrance of the pipe. Fig. 7 shows the time history response of the obtained sound pressure, while Fig. 8 shows the Fourier spectrum of the sound pressure level. A very large and steep peak is detected around 0.005 s. This peak is the signal of the traveling wave of sound generated by a point sound source (acoustic impulse) via an LIP with a microphone. Thereafter, a peak appears periodically. The sound wave generated via an LIP is reflected by the end of the pipe and is re-measured by the microphone. The acoustic mode is excited up to a band of 3 kHz (Fig. 8). Each peak in the Fourier spectrum is generated at the resonance frequency of each mode of the sound field. Table 1 compares the theoretical resonance frequencies up to the 16th order of the pipe subjected to an open-end correction and the measured peak frequency in the Fourier spectrum. The theoretical value of the resonance frequency f_n is given by Eq. (5) [29].

$$f_n = \frac{nc}{2L} \tag{5}$$

Here, n is the mode order, L [m] is the total pipe length, and c [m/s] is the sound velocity. The sound velocity is determined by Eq. (6).

$$c = \sqrt{\frac{\kappa R_0 T}{M}} \tag{6}$$

Here, κ is the specific heat ratio, M [kg/mol] is the air molecular weight, R_0 [J/mol K] is the general gas constant, and T [K] is the temperature. The total pipe length is defined by Eq. (7).

$$L = l + 2\Delta l \tag{7}$$

Here, l is the pipe length, and Δl is the open-end correction and is given by Eq. (8), where the pipe inner radius is r [m].

$$\Delta l = 0.61r \tag{8}$$

The present experiment is carried out at a temperature of $T = 289.2$ K. The calculated theoretical value of the resonance frequency is shown in Table 1. The theoretical values and the measured values agree well, indicating that the system can realize a highly reliable measurement. The results in Table 1 and Fig. 8 confirm that the measurement is performed only in the acoustic mode in this experimental apparatus. Hence, the structural vibration of the pipe does not affect the acoustic characteristics and no component of the structural vibration is included, even in Fig. 7.

5.2. Acoustic characteristics in healthy and damaged (hole) conditions

Fig. 9 shows the outline and dimensions of an acrylic pipe with a hole. The diameter of the hole is 6 mm. Fig. 10 shows the time history responses of the sound pressure measured in the healthy pipe and the damaged pipe. It should be noted that

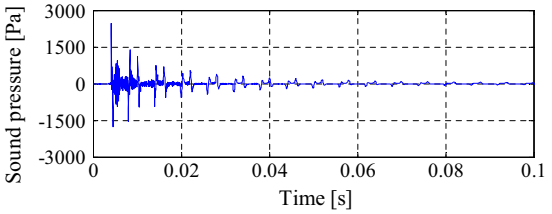

Fig. 7. Time response of the sound pressure.

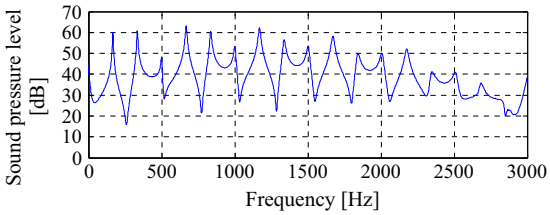

Fig. 8. Fourier spectrum of the sound pressure.

Table 1
Comparison of the theoretical and experimental mode frequencies.

Mode	Theoretical value [Hz]	Experimental value [Hz]	Error [%]
1	168.6	165.6	1.78
2	337.1	332.8	1.28
3	505.7	498.4	1.44
4	674.2	667.2	1.04
5	842.8	834.4	1.00
6	1011	1000	1.09
7	1180	1169	0.93
8	1348	1338	0.74
9	1517	1502	0.99
10	1686	1670	0.95
11	1854	1841	0.70
12	2023	2005	0.89
13	2191	2175	0.73
14	2360	2350	0.42
15	2528	2506	0.87
16	2697	2683	0.52

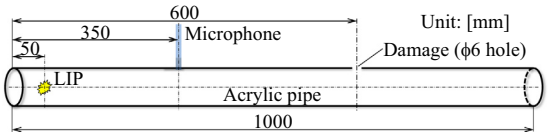

Fig. 9. Objective pipe structure with damage.

Fig. 10(a) and (b) have different time scales. In the healthy pipe without damage, peaks occur periodically (Fig. 10(a)). The periodicity is attributed to the numerous reflections at the end of the pipe, which are measured several times by the microphone. In Fig. 10(b), T_a is the time when the impulse is first inputted, and T_b is the time when the next peak is generated. Herein T_a = 9.927 ms and T_b = 13.79 ms. The result when applying the continuous wavelet (Fig. 11(a)) indicates that the wavelet coefficients become larger at T_a and T_b, and characteristic signals are captured at these times. Since the moving time of the sound wave is $\Delta T = T_b - T_a = 3.863$ ms, multiplying the sound speed ($c = 341.2$ m/s) produces the moving distance of the sound wave of $l' = \Delta T \times c = 1.318$ m. The to-and-fro of the distance from the actual microphone to the end of the pipe is 1.320 m, including the open-end correction, which is almost the same value. Thus, Fig. 10 confirms that the time history response is correctly measured but determining the characteristic differences in the properties between the healthy pipe and the damaged pipe is difficult.

5.3. Damage detection using a continuous wavelet transform

Based on the concept described in Section 4.3, a continuous wavelet transform is applied to the measured acoustic data to detect damage and identify its position. The calculations are performed using one-dimensional continuous wavelet conversion commands in numerical calculation software MATLAB and its application Wavelet Toolbox. Fig. 11 shows the result of applying the continuous wavelet transform. Fig. 11(a) shows the results of applying a continuous wavelet transform to the time history response of the sound pressure measured for a healthy pipe. Fig. 11(b) shows the result for a damaged pipe. The horizontal axis in Fig. 11(a) and (b) represents time, while the vertical axis represents scale parameter a, and the color map represents the largeness of a wavelet coefficient $W(a, b)$. In the color map, the brighter a portion is, the larger the absolute value of the wavelet coefficient $W(a, b)$, which denotes a local change in the signal. In addition, the darker a portion is, the

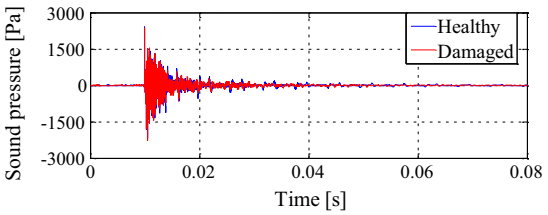

(a) Time [0-0.08 s]

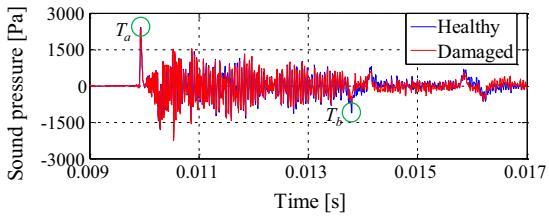

(b) Time [0.009-0.017 s]

Fig. 10. Time responses in healthy and damaged (hole) conditions.

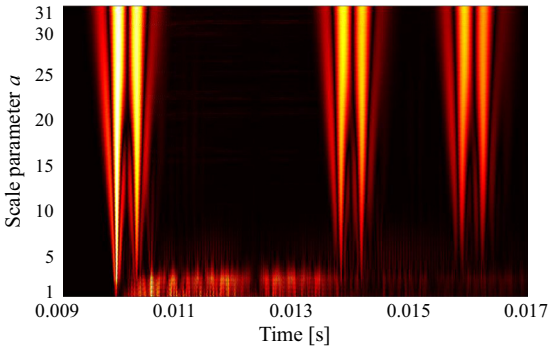

(a) Wavelet coefficient in the healthy condition

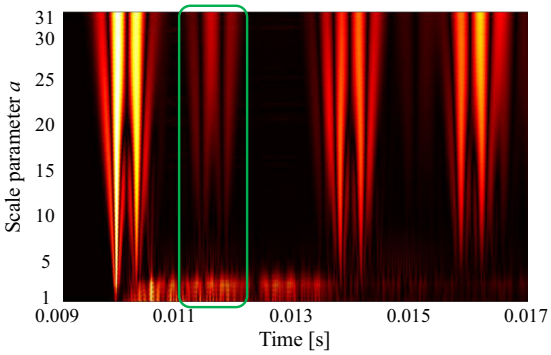

(b) Wavelet coefficient in the damaged (hole) condition

Fig. 11. Wavelet transform in healthy and damaged (hole) conditions.

smaller the absolute value, indicating a cyclic signal or a signal with a small value. Comparing the time history response in Fig. 10(b) with the wavelet application result in Fig. 11(a) leads to a feature where the sound wave is reflected at the end of the pipe and the absolute value of the wavelet coefficient increases according to the peak generated when the wave is measured again by the microphone (i.e., a brighter portion appears periodically). The wavelet coefficient shown in Fig. 11(a) similarly appears in (b). The portion surrounded by a green frame in Fig. 11(b) does not appear in (a). Since the difference in the experimental conditions between Fig. 11(a) and (b) is the presence of a hole drilled in the pipe, the difference in the signal is attributed to the reflection of the sound wave due to the damage.

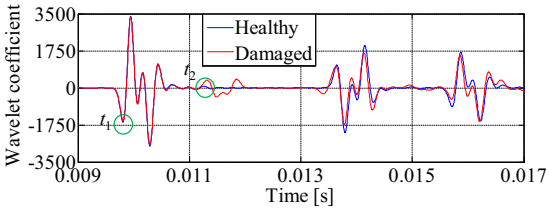

Fig. 12. Wavelet coefficients ($a = 16$).

Cutting the color map in Fig. 11 in the vertical direction with an arbitrary scale parameter gives the characteristics of the wavelet coefficient with respect to the scale parameter. The difference between the pipe characteristics with and without damage leads to a position identification of damage in the pipe. In this case, a portion with the scale parameter $a = 16$ is cut.

Although the aforementioned color map shows the absolute values of the wavelet coefficients, Fig. 12 provides the numerical values. Fig. 12 shows the characteristics of the wavelet coefficients for $a = 16$. The horizontal and vertical axes represent the time and wavelet coefficients, respectively. The diagram up to 0.011 s shows almost the same wavelet values for both the healthy condition and the damaged (hole) condition. However, fluctuations occur only for the damaged (hole) condition after 0.011 s. The time is almost the same as the time indicated by a green frame in Fig. 11(b).

As shown in Fig. 12, t_1 denotes the time when the first fluctuation occurs in both cases and t_2 indicates the time where only a fluctuation due to the hole occurs. Thus, the distance traveled by a sound wave during these times is examined. Since $t_1 = 9.810$ ms and $t_2 = 11.30$ ms, the traveling time of sound wave is $\Delta t = t_2 - t_1 = 1.490$ ms. Accordingly, multiplying the difference by the speed of sound produces $\Delta L = \Delta t \times c = 0.5084$ m. In Fig. 9, the to-and-fro distance between the microphone and the hole is 0.5 m, which is almost equal to the value obtained above. As a result, the effectiveness of this method to extract the difference in the acoustic characteristics by the presence or absence of a hole via continuous wavelet transform and to identify the damaged position is demonstrated.

6. Conclusions

A change in a pipe's characteristics due to drill damage may be extracted via an acoustic excitation using a laser-induced plasma generated by a high-power pulse laser and applying a wavelet transform to the time history response of the sound pressure obtained by acoustic measurements using a microphone. Furthermore, appropriately selecting a scale parameter and extracting the reflected sound due to damage may accurately identify the damaged position. With this method, device placement for excitation in a structure is unnecessary. The presence of damage is accurately determined and the location of damage is easily identified. Consequently, this method greatly contributes to maintaining the health of a system.

In this experiment, the laser output is 600 mJ. Increasing the laser output can improve the sound pressure level of the acoustic excitation input. Consequently, the acoustic excitation method and the proposed damage detection method can be applied to a larger pipe structure. Because this method can also detect a smaller pipe structure in lifelines as well as damage in arbitrary space (e.g., peeling or missing object), the proposed method has potential for diverse applications. By contrast, when it is difficult to generate the laser-induced plasma inside a pipe, a pulsed laser can be directly irradiated onto the pipe surface (outer surface), and a similar damage detection may be possible by acting as an impulse excitation force on the structure by laser ablation generated and measuring the acoustic or structural vibration characteristics caused by the impulse excitation force.

In the future, we will evaluate this method under conditions of various target structures and excitation points/measurement points and expand its applicability to arbitrary test objects. Furthermore, we will quantitatively evaluate the ability of the wavelet coefficients to extract damage and to detect size and distance of damage.

Acknowledgements

We thank the Japan Society for the Promotion of Science for their support under Grants-in-Aid for Scientific Research programs (Grants-in-Aid for Scientific Research (B), Project No. JP16H04286 and No. JP16H04291, and Grant-in-Aid for Challenging Exploratory Research, Project No. JP17K18858).

References

[1] R.D. Sante, Fibre optic sensors for structural health monitoring of aircraft composite structures: recent advances and applications, Sensors 15 (2015) 18666–18713.
[2] D.M. Peairs, G. Park, D.J. Inman, Improving accessibility of the impedance-based structural health monitoring method, Intell. Mater. Syst. Struct. 15 (2004) 129–139.
[3] S. Ritdumrongkul, M. Abe, Y. Fujino, T. Miyashita, Quantitative health monitoring of bolted joints using a piezoceramic actuator sensor, Smart Mater. Struct. 13 (2004) 20–29.
[4] I. Argatov, I. Sevostianov, Health monitoring of bolted joints via electrical conductivity measurements, Int. J. Eng. Sci. 48 (2010) 874–887.

[5] M.D. Todd, J.M. Nichols, C.J. Nichols, L.N. Virgin, An assessment of modal property effectiveness in detecting bolted joint degradation: theory and experiment, J. Sound Vib. 275 (2004) 1113–1126.
[6] F. Huda, I. Kajiwara, N. Hosoya, S. Kawamura, Bolt loosening analysis and diagnosis by non-contact laser excitation vibration tests, Mech. Syst. Signal Process. 40 (2013) 589–604.
[7] X. Jing, K.-Y. Fung, Generation of desired sound impulses, J. Sound Vib. 297 (2006) 61–626.
[8] H. Shibayama, K. Fukunaga, K. Kido, Directional characteristics of pulse sound source with spark discharge, J. Acoust. So. Jpn. (E) 6 (1985) 73–77.
[9] Y.E. Krasik, A. Grinenko, A. Sayapin, S. Efimov, A. Fedotov, V.Z. Gurovich, V.I. Oreshkin, Underwater electrical wire explosion and its applications, IEEE Trans. Plasma Sci. 36 (2008) 423–434.
[10] Y. Ying, J. Harley, J.H. Garrett, Jr., José M.F. Moura, N. O'Donoughue, I.J. Oppenheim, L. Soibelman, Time reversal for damage detection in pipes, in: Proc. SPIE 7647, Sensors and Smart Structures Technologies for Civil, Mechanical, and Aerospace Systems, 2010, pp. 76473S.
[11] A. Demma, P. Cawley, M. Lowe, A.G. Roosenbrand, B. Pavlakovic, The reflection of guided waves from notches in pipes: a guide for interpreting corrosion measurements, NDT and E Int. 37 (2004) 167–180.
[12] M.J.S. Lowe, D.N. Alleyne, P. Cawley, Defect detection in pipes using guided waves, Ultrasonics 36 (1998) 147–154.
[13] I. Buethe, M.A. Torres-Arredondo, L.-E. Mujica, J. Rodellar, C.-P. Fritzen, Damage detection in piping systems using pattern recognition techniques, in: Proceedings of 6th European Workshop on Structural Health Monitoring, Fr.1.D.3, 2012, pp. 1–8.
[14] I. Kajiwara, N. Hosoya, Vibration testing based on impulse response excited by laser ablation, J. Sound Vib. 330 (2011) 5045–5057.
[15] N. Hosoya, I. Kajiwara, T. Hosokawa, Vibration testing based on impulse response excited by pulsed-laser ablation: measurement of frequency response function with detection-free input, J. Sound Vib. 331 (2012) 1355–1365.
[16] N. Hosoya, I. Kajiwara, T. Inoue, K. Umenai, Non-contact vibro-acoustic tests based on nanosecond laser ablation, J. Sound Vib. 333 (2014) 4254–4264.
[17] N. Hosoya, R. Umino, I. Kajiwara, S. Maeda, T. Onuma, A. Mihara, Damage detection in transparent materials using non-contact laser excitation by nano-second laser ablation and polarization high-speed camera, Exp. Mech. 56 (2016) 339–343.
[18] N. Hosoya, I. Kajiwara, K. Umenai, Dynamic characterizations of underwater structures using non-contact vibration test based on nanosecond laser ablation in water: investigation of cavitation bubbles by visualizing shockwaves using the Schlieren method, J. Vib. Control 22 (17) (2016) 3649–3658.
[19] N. Hosoya, R. Umino, A. Kanda, I. Kajiwara, A. Yoshinaga, Lamb wave generation using nanosecond laser ablation to detect damage, J. Vib. Control, Epub ahead of print 19 January 2017. http://doi.org/10.1177/1077546316687904.
[20] N. Hosoya, I. Kajiwara, K. Umenai and S. Maeda, Dynamic characterizations of underwater structures using noncontact vibration tests based on nanosecond laser ablation in water: evaluation of passive vibration suppression with damping materials, J. Vib. Control, Epub ahead of print 18 May 2017. http://doi.org/10.1177/1077546317710158.
[21] M. Oksanen, J. Hietanen, Photoacoustic breakdown sound source in air, Ultrasonics 32 (1994) 327–331.
[22] Q. Qin, K. Attenborough, Characteristics and application of laser-generated acoustic shockwaves in air, Appl. Acoust. 65 (2004) 325–340.
[23] V.B. Georgiev, V.V. Krylov, Q. Qin, K. Attenborough, Generation of flexural waves in plates by laser-initiated airborne shock waves, J. Sound Vib. 330 (2011) 217–228.
[24] J.G. Bolaños, V. Pulkki, P. Karppinen, E. Hæggström, An optoacoustic point source for acoustic scale model measurements, J. Acoust. Soc. Am. 133 EL221–EL227.
[25] N. Kawahara, J.L. Beduneau, T. Nakayama, E. Tomita, Y. Ikeda, Spatially, temporally, and spectrally resolved measurement of laser-induced plasma in air, Appl. Phys. B: Lasers Opt. 86 (2007) 605–614.
[26] D. Bradley, C.G.W. Sheppard, I.M. Suardjaja, R. Woolley, Fundamentals of high-energy spark ignition with lasers, Combust. Flame 138 (2004) 55–77.
[27] F. Ferioli, S.G. Buckley, Measurements of hydrocarbons using laser-induced breakdown spectroscopy, Combust. Flame 144 (2006) 435–447.
[28] R. Petkovšek, D. Horvat, G. Močnik, M. Terzić, J. Možina, Analysis of optodynamic sources generated during laser-induced breakdown in water, Ultrasonic 44 (2006) 1255–1258.
[29] N. Hosoya, M. Nagata, I. Kajiwara, Acoustic testing in a very small space based on a point sound source generated by laser-induced breakdown: stabilization of plasma formation, J. Sound Vib. 332 (2013) 4572–4583.
[30] N. Hosoya, M. Nagata, I. Kajiwara, R. Umino, Nano-second laser-induced plasma shock wave in air for non-contact vibration testing, Exp. Mech. 56 (2016) 1305–1311.
[31] Y. Zhang, T. Hiruta, I. Kajiwara, N. Hosoya, Active vibration suppression of membrane structures and evaluation with a non-contact laser excitation vibration test, J. Vib. Control 23 (2017) 1681–1692.
[32] N. Hosoya, M. Mishima, I. Kajiwara, S. Maeda, Non-destructive firmness assessment of apples using a non-contact laser excitation system based on a laser-induced plasma shock wave, Postharvest Biol. Technol. 128 (2017) 11–17.
[33] F. Huda, I. Kajiwara, N. Hosoya, Damage detection in membrane structures using non-contact laser excitation and wavelet transformation, J. Sound Vib. 333 (2014) 3609–3624.
[34] C. Zeng, H. Lin, Q. Jiang, M. Xu, QRS complex detection using combination of Mexhican-hat wavelet and complex morlet wavelet, J. Comput. 8 (11) (2013) 2951–2958.